

Strong Baseline: Multi-UAV Tracking via YOLOv12 with BoT-SORT-ReID

Yu-Hsi Chen

The University of Melbourne
Parkville, Australia

yuhsi@student.unimelb.edu.au

Abstract

Detecting and tracking multiple unmanned aerial vehicles (UAVs) in thermal infrared video is inherently challenging due to low contrast, environmental noise, and small target sizes. This paper provides a straightforward approach to address multi-UAV tracking in thermal infrared video, leveraging recent advances in detection and tracking. Instead of relying on the YOLOv5 with the DeepSORT pipeline, we present a tracking framework built on YOLOv12 and BoT-SORT, enhanced with tailored training and inference strategies. We evaluate our approach following the metrics from the 4th Anti-UAV Challenge and demonstrate competitive performance. Notably, we achieve strong results without using contrast enhancement or temporal information fusion to enrich UAV features, highlighting our approach as a "Strong Baseline" for the multi-UAV tracking task. We provide implementation details, in-depth experimental analysis, and a discussion of potential improvements. The code is available at <https://github.com/wish44165/YOLOv12-BoT-SORT-ReID>.

1. Introduction

Multi-UAV tracking has emerged as a crucial application in recent years, driven by significant advancements in hardware, detection models, and tracking algorithms. As UAVs equipped with sophisticated visual systems and advanced control dynamics continue to proliferate, a wide range of UAV-based products have been introduced, as presented in [29]. However, these innovations also introduce new challenges, particularly in tracking UAV swarms. The need for effective swarm tracking has become increasingly urgent due to growing security concerns and the rising threat posed by unauthorized UAVs. Various UAV-related datasets have been developed to address these challenges to advance tracking and detection tasks. These datasets include trajectory reconstruction datasets, such as those in [14, 21], which provide UAV trajectories captured from single or multi-view cameras, and trajectory-based UAV datasets in-

roduced in [3]. Additionally, RGB-based footage datasets, including those in [20, 30, 32, 34], have been widely used. Among these, thermal infrared video-based UAV datasets featuring both single-object tracking (SOT) and multi-object tracking (MOT) scenarios in [13, 17], have gained significant attention, particularly in major challenge events. These datasets have played a pivotal role in improving UAV tracking and detection capabilities.

Thermal infrared videos offer advantages over traditional RGB imagery, such as enhanced visibility in low-light and adverse weather conditions, making them ideal for security and surveillance applications. This paper focuses on using thermal infrared video for multi-UAV tracking, exploiting its importance in challenging environments where RGB-based methods may fail. Fig. 1 (a) illustrates thermal infrared frames with diverse backgrounds from the MOT training set, while Fig. 1 (b) highlights minor defects, such as annotation errors, redundancies, missed labels, and low-quality frames, that account for a negligible portion of the dataset and can be safely disregarded during training. Additionally, Fig. 2 displays cropped image patches from bounding box annotations in the training set, illustrating the varying sizes of UAVs, from several pixels to single-digit pixels. We build a complete UAV tracking workflow by leveraging the latest YOLOv12 [36] detector and BoT-SORT [1] tracking algorithm, which outperform the well-established YOLOv5 [18] with DeepSORT [40] combination. We also implement some strategies to enhance multi-UAV tracking performance further. Our contributions are as follows:

1. We establish a multi-UAV tracking workflow based on YOLOv12 and BoT-SORT, setting a strong baseline for thermal infrared video-based multi-UAV tracking tasks.
2. We provide insightful analysis of various trial adjustments, such as the impact of input image size and tracker buffer tuning, and offer essential considerations for future improvements starting from our strong baseline.

2. Related Work

Existing perspectives for improving thermal infrared video-based multi-UAV tracking can be categorized into annota-



Figure 1. Demonstration using training and testing data from Track 3. (a) Shows UAV swarms with varying sizes and backgrounds in the training data. (b) Highlights annotation errors and frame defects: MultiUAV-230 (train) has incorrect annotations, MultiUAV-256 (train) contains redundant annotations, MultiUAV-294 (train) has missed annotations, and MultiUAV-068 (test) includes a poor-quality frame.

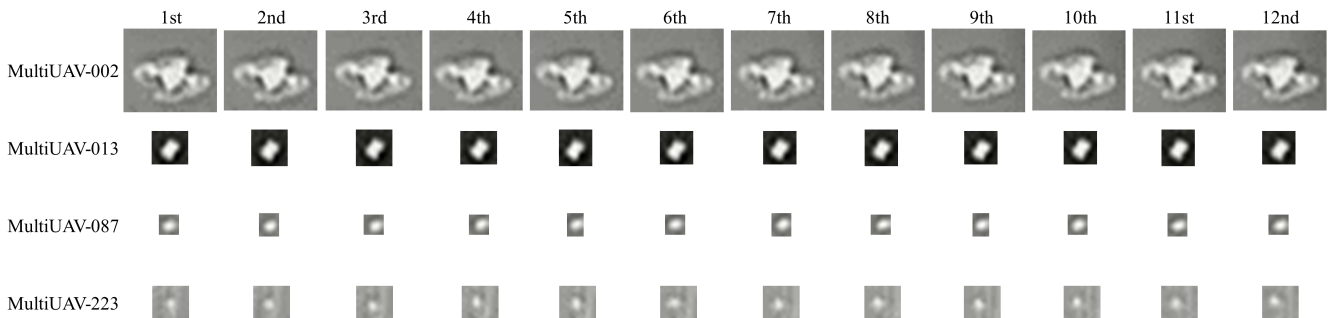


Figure 2. Illustration of cropped image patches from training data annotations. Each patch corresponds to a bounding box from MultiUAV-002, MultiUAV-013, MultiUAV-087, and MultiUAV-223, with sizes approximately 28×24 , 10×10 , 6×6 , and 11×10 , respectively. The top number denotes the frame sequence (1st to 12th frames), and each row represents the same object (same ID across frames).

tion and benchmarking, spatial information enhancement, temporal and motion modeling, real-time optimization, unified frameworks, and detection-based tracking systems. As high-quality annotation is fundamental for robust tracking, prior studies have examined the impact of annotation errors on object detection [19], incorporated Multiple Hypothesis Tracking (MHT) to leverage temporal cues and reduce false positives [15], and introduced benchmarks to evaluate

detection and tracking methods on UAV datasets [16]. Spatial information enhancement techniques, such as the Image Pyramid Guidance (IPG) module presented in [23], address feature imbalance by preserving fine-grained spatial details for accurate bounding box regression and classification, even in deep network layers.

To further improve tracking robustness, temporal and motion modeling techniques exploit inter-frame correla-

tions, enhancing continuity and reducing fragmentation [11, 12, 22, 42]. Complementary to this, real-time optimization strategies reduce inference latency while maintaining accuracy, enabling efficient UAV tracking in real-world applications [7, 26, 39, 41]. Beyond these, unified frameworks integrate detection and tracking into end-to-end solutions, streamlining multi-UAV tracking pipelines [44, 46]. Additionally, detection-based methods incorporating cascading post-processing modules refine tracking accuracy by mitigating false positives and improving localization [35]. While prior works have contributed significantly to multi-UAV tracking, our approach advances the field by leveraging the latest detector and tracker, setting a new benchmark for thermal infrared video-based UAV tracking and guiding future research in the multi-UAV tracking task.

3. Methodology

This section first defines the problem scope, followed by data analysis and preparation for model training. We then introduce the primary detection model, YOLOv12, and the tracking algorithm, BoT-SORT, before detailing our training and inference strategies.

3.1. Problem Statement

The goal is to track UAVs as accurately as possible, with evaluation metrics detailed in Sec. 4.1. The challenge consists of three tracks, each corresponding to a different scenario. Track 1 and Track 2 are SOT tasks, differing in whether the UAV’s initial location is given. Track 3 is a MOT task where the initial locations of UAVs are provided.

3.2. Data Analysis and Preparation

We first analyze each track’s training and testing data, as summarized in Tab. 1. Track 1 and Track 2 share the same training set, consisting of 23 sequences at 512×512 resolution and 200 sequences at 640×512 resolution. The training set for Track 3 is composed of 200 sequences at 640×512 resolution. For testing, Track 1 and Track 2 each contain 216 non-overlapping sequences. Track 1’s test set is entirely at 640×512 resolution, while Track 2 includes 16 sequences at 640×512 and 200 at 512×512 . Track 3’s test set consists of 100 sequences at 640×512 resolution. Additionally, Tab. 1 reports the width, height, and area distributions, along with their mean and standard deviation, providing essential insights for model hyperparameter tuning. Note that there may be slight differences in the numbers compared to the official release, as we have removed redundant annotations and defect cases, as illustrated in Fig. 1 (b).

After analyzing the data, we split it for model training preparation. The number of frames and bounding boxes used for training, validation, and testing in the SOT and MOT tasks are detailed in Tab. 2. Specifically, Track 1 and Track 2 use YOLOv12 with BoT-SORT, while Track 3

employs YOLOv12 with BoT-SORT-ReID. Note that some numbers are in parentheses since we found the test set to provide limited information for the SOT task. Thus, the values in parentheses reflect the data only split into training and validation sets. Additionally, for BoT-SORT training, 1/10 of the data is primarily used to train the ReID module. This approach provides more effective ReID module training since many scenes are visually similar.

3.3. YOLOv12 with BoT-SORT-ReID for MOT

Based on the comprehensive evaluation results presented in [3], which benchmarks the YOLO series of detectors on UAV datasets featuring RGB footage, YOLOv12 was selected for all tracks due to its superior performance. YOLOv12 [36] represents the latest advancement in the YOLO series of object detectors, introducing key innovations to enhance accuracy and efficiency simultaneously. At its core, YOLOv12 adopts the Residual Efficient Layer Aggregation Network (R-ELAN), which addresses the optimization challenges associated with attention mechanisms, particularly in large-scale models. Building upon ELAN [37], R-ELAN introduces a block-level residual design with adaptive scaling alongside a refined feature aggregation strategy, jointly promoting effective feature reuse and stable gradient propagation with minimal overhead. Furthermore, YOLOv12 integrates an attention-centric architecture by combining FlashAttention [5, 6] with spatially aware modules, enabling enhanced contextual modeling while preserving low latency. Introducing 7×7 large-kernel separable convolutions broadens the receptive field and strengthens object localization, particularly for small and medium-sized targets. The architecture is optimized for modern GPU memory hierarchies, delivering improved computational efficiency and reduced inference times without compromising detection performance. These innovations enable YOLOv12 to balance speed and accuracy, making it highly suitable for real-time applications, large-scale detection tasks, and tracking pipelines.

BoT-SORT [1] combines a Kalman Filter [40] with camera motion compensation (CMC) to stabilize tracking under dynamic conditions. CMC employs global motion compensation (GMC) via affine transformations, using image keypoints [33] tracked with pyramidal Lucas-Kanade optical flow [2] and outlier rejection. The affine transformation, estimated via RANSAC [8], compensates for background motion while maintaining object trajectory stability by adjusting Kalman Filter state vectors. BoT-SORT-ReID enhances multi-object tracking by integrating appearance cues from four distinct ReID architectures. The Bag of Tricks (Bagtricks) baseline employs a ResNet-50 backbone with batch normalization, triplet loss, and cross-entropy loss for robust feature extraction. Attention Generalized-Mean Pooling with Weighted Triplet Loss (AGW) [43] improves

Characteristic	Training Data			Testing Data		
	Track 1	Track 2	Track 3	Track 1	Track 2	Track 3
Number of Sequences	23 / 200		200	216	16 / 200	100
Number of Frames	16,022 / 231,557		151,831	232,742	11,619 / 221,123	75,487
Resolutions	512×512 / 640×512		640×512	640×512	512×512 / 640×512	640×512
Total Bounding Boxes	229,839		3,127,045	216	0	2,041
Width Range (px)	[1, 146]		[0.96, 98.92]	[4, 140]	N/A	[1.86, 28.33]
Width Mean ± Std (px)	30.55 ± 24.43		10.56 ± 5.75	40.56 ± 26.34	N/A	9.71 ± 4.06
Height Range (px)	[1, 131]		[0.57, 55.5]	[3, 68]	N/A	[2.44, 25.78]
Height Mean ± Std (px)	19.43 ± 13.63		9.06 ± 4.67	23.76 ± 13.34	N/A	8.56 ± 3.55
Area Range (px ²)	[1, 17,161]		[0.95, 4344.63]	[16, 7,956]	N/A	[10.88, 575.41]
Area Mean ± Std (px ²)	874.91 ± 1158.50		119.05 ± 179.40	1241.12 ± 1280.20	N/A	95.14 ± 86.91

Table 1. Summary of data characteristics for training and testing. The training data for Track 1 and Track 2 are identical, while the testing data for Track 1 and Track 2 have no overlapping parts. Since Track 2 does not provide initial bounding boxes, we use "N/A" to indicate that this information is not applicable. Note that some bounding boxes were removed in Track 1 and Track 2 training sets due to labeled non-existent, zero-sized width or height, and cases where the boxes covered the entire image.

Characteristic	Single-Object Tracking			Multi-Object Tracking			
	YOLOv12			YOLOv12		BoT-SORT-ReID	
	Train	Valid	Test	Train	Valid	Train	Valid
Number of Frames	148,547 (198,063)	49,515 (49,516)	49,517	121,355	30,337	75,913 (7,593)	75,918 (7,783)
Total Bounding Boxes	138,084 (184,056)	45,848 (45,921)	46,045	2,501,753	625,292	1,580,931 (155,833)	1,546,092 (160,876)

Table 2. Data preparation summary for YOLOv12 and BoT-SORT-ReID across single-object (Track 1 and Track 2) and multi-object (Track 3) tracking. For YOLOv12 in SOT, numbers in parentheses indicate an alternative split with only training and validation sets. For BoT-SORT-ReID, numbers in parentheses indicate a reduced ReID training set selecting only the first 1/10 of frames from each sequence.

feature representation by incorporating non-local modules and generalized mean pooling. Strong Baseline (SBS) [25] enhances robustness with generalized mean pooling, circle softmax loss, and an advanced data augmentation strategy. Multiple Granularity Network (MGN) [38] extends SBS by introducing multiple feature branches to capture fine-grained representations across different spatial scales. Additionally, linear tracklet interpolation with a 20-frame gap, following ByteTrack [45], mitigates missed detections from occlusions or annotation errors.

3.4. Training and Inference Strategies

To reduce the training time of the YOLOv12 detector, we adopt a two-stage training strategy. First, we train YOLOv12 models (n, s, m, l, x) from scratch on the SOT dataset, which is split into training, validation, and testing subsets as detailed in Tab. 2. Subsequently, starting from this checkpoint, we fine-tune these models on the MOT dataset or with larger input image resolutions. This staged approach accelerates convergence, reduces overall training time, and enables the model to achieve competitive Average Precision (AP) within just a few epochs. For the ReID module, we primarily employ a reduced subset of the dataset to enhance training efficiency, as using the entire dataset for

training would be highly time-consuming.

The inference workflow is presented in Fig. 3. The overall procedure follows the original BoT-SORT scheme. However, we modify the output by reporting both online and lost targets for Track 1 and Track 2 while preserving the original output format for Track 3. We did not use linear track interpolation because ID switching frequently occurs due to camera motion or fast-moving UAVs, making interpolation ineffective for recovering missing detections. Instead, for the SOT task, we adopt a strategy based on the assumption that each frame contains at most one UAV, following this priority order: (1) report the UAV with the highest confidence score among the online targets, (2) if no online target is available, continue reporting the previous ID as the lost target in the subsequent tracker buffer frames, (3) if no previous ID is available, report the last known location until new online targets are detected. This strategy leverages the Kalman Filter’s prediction to accurately estimate the UAV’s location based on prior positions and velocity, significantly improving evaluation metrics in the SOT task. However, this strategy is not feasible for the MOT task due to the frequent overlap and ID switching between online and lost targets, which would lead to poor results. Therefore, we maintain the original output for Track 3 in this case.

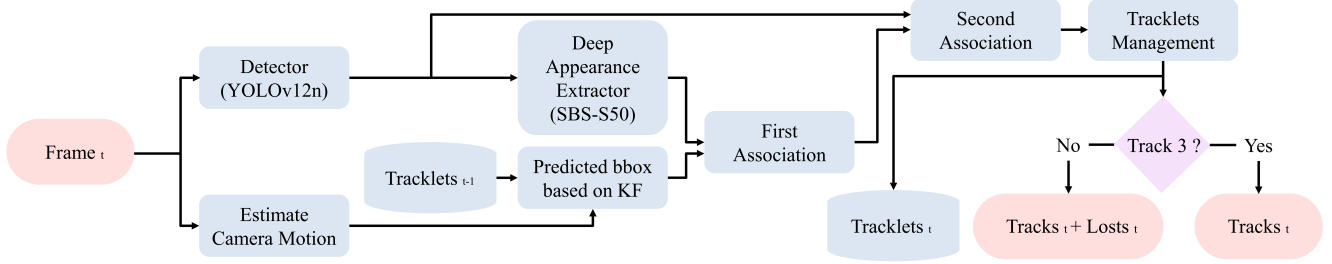


Figure 3. YOLOv12n with BoT-SORT-SBS-S50 workflow diagram. The workflow follows the original BoT-SORT framework [1], with a slight revision: incorporating lost tracks to compensate for uninformative frames and improve object continuity. Specifically, for Track 1 and Track 2, lost target information is used to annotate potential object locations, while Track 3 retains the BoT-SORT original output.

4. Experimental Results

The experiments were conducted on two platforms: the first, a system with an Intel Core i7-12650H CPU, an NVIDIA RTX 4050 GPU, and 16 GB of RAM; the second, a high-performance computing (HPC) system [27], equipped with an NVIDIA H100 GPU and 80 GB of memory. All models were trained using the default settings (*e.g.*, image input size of 640 and a track buffer of 30 frames) unless otherwise specified in the content or tables. This section begins by outlining the evaluation metrics for the three tracks, followed by the results for both the SOT and MOT tasks. We then present the leaderboard rankings and discuss key considerations and potential image enhancement techniques that could further improve UAV tracking.

4.1. Evaluation Metrics

Two evaluation metrics are used across the three competition tracks. The first metric applies to Track 1 and Track 2, where tracking accuracy is defined as:

$$\text{acc} = \sum_{t=1}^T \frac{\text{IoU}_t \cdot \delta(v_t > 0) + p_t \cdot (1 - \delta(v_t > 0))}{T} - 0.2 \cdot \left(\sum_{t=1}^{T^*} \frac{p_t \cdot \delta(v_t > 0)}{T^*} \right)^{0.3}. \quad (1)$$

Here, IoU_t is the Intersection over Union between the predicted and ground-truth bounding boxes at frame t . The variable p_t denotes the predicted visibility flag, where $p_t = 1$ if the predicted box is empty, and $p_t = 0$ otherwise. The ground-truth visibility is given by v_t , and $\delta(v_t > 0)$ is an indicator function that equals 1 when the target is visible ($v_t > 0$) and zero otherwise. The accuracy is averaged over all T frames, with T^* representing the number of frames in which the target is visible in the ground truth. The second metric used for Track 3 is the Multi-Object Tracking Accuracy (MOTA), which jointly penalizes false positives (FP), false negatives (FN), and identity switches (IDS), normal-

ized by the total number of ground-truth objects (GT):

$$\text{MOTA} = 1 - \frac{\text{FP} + \text{FN} + \text{IDS}}{\text{GT}}. \quad (2)$$

MOTA ranges from $-\infty$ to 1, with higher values indicating better tracking performance. The final score is obtained by averaging MOTA over all sequences. The following sections will present and evaluate all performance results based on the abovementioned metrics.

4.2. Evaluation Results on Track 1 and Track 2

We present the evaluation results for Track 1 and Track 2 together, as both are SOT tasks, with the only difference being the presence of the initial UAV location. Eight meaningful trials are selected for both tracks, as shown in Tab. 3. Trials 1 and 2 serve as an ablation study to assess the impact of BoT-SORT. The results demonstrate a significant performance improvement: the score in Track 1 increases from 0.0786 to 0.5529, and in Track 2, it rises from 0.0992 to 0.3106 simply by adding BoT-SORT after the YOLOv12n detector. Trials 2 through 6 evaluate different detector model sizes (n, s, m, l, x), with the highest score achieved using YOLOv12l for both tracks. Trial 7 examines the effect of extended 300 epochs training, revealing a decline in performance compared to the 100 epochs training, likely due to overfitting. Finally, Trial 8 for each track shows the highest score we submitted, tuning the minimum bounding box area threshold from 10 to 4 for Track 1 and from 10 to 1 for Track 2 to better capture smaller UAVs that may have been missed with the default setting.

4.3. Evaluation Results on Track 3

The evaluation results for Track 3 can be categorized into four key observations. As shown in Tab. 4, Group 1 presents results using various YOLOv12 model sizes, revealing that YOLOv12n achieves the best performance despite being the smallest model. Group 2 examines the effect of different track buffer sizes, with the highest score observed using 60 buffer frames, suggesting that this configuration optimizes

Configurations	Track 1								Track 2							
	Trial 1	Trial 2	Trial 3	Trial 4	Trial 5	Trial 6	Trial 7	Trial 8	Trial 1	Trial 2	Trial 3	Trial 4	Trial 5	Trial 6	Trial 7	Trial 8
YOLOv12	n	n	s	m	l	x	x	n	n	n	s	m	l	x	x	n
- epochs	100	100	100	100	100	100	300	100	100	100	100	100	100	100	300	100
BoT-SORT	✗	✓	✓	✓	✓	✓	✓	✓	✗	✓	✓	✓	✓	✓	✓	✓
- min box area	10	10	10	10	10	10	10	4	10	10	10	10	10	10	10	1
Scores	0.0786	0.5529	0.5637	0.5634	0.5644	0.5548	0.5398	0.5813	0.0992	0.3106	0.3258	0.3283	0.3285	0.3132	0.3080	0.3559

Table 3. Evaluation results for Track 1 and Track 2, summarizing eight trials per track. The first two rows detail YOLOv12 configurations, varying model sizes (n, s, m, l, x), and training epochs. The third row specifies the use of BoT-SORT (“✗” indicates exclusion; “✓” indicates inclusion). The fourth row lists the “min box area” threshold for filtering tiny bounding boxes, adjusted to 4 and 1 to account for tiny UAVs. The final row reports the resulting scores.

Configurations	Group 1					Group 2				
	Trial 1	Trial 2	Trial 3	Trial 4	Trial 5	Trial 6	Trial 7	Trial 8	Trial 9	Trial 10
YOLOv12	n	s	m	l	x	n	n	n	n	n
BoT-SORT	✓	✓	✓	✓	✓	✓	✓	✓	✓	✓
- track buffer	30	30	30	30	30	15	45	60	75	90
Scores	0.638763	0.635361	0.633887	0.631864	0.630822	0.638609	0.638781	0.638801	0.638788	0.638771

Configurations	Group 3		Group 4							Final
	Trial 11	Trial 12	Trial 13	Trial 14	Trial 15	Trial 16	Trial 17	Trial 18	Trial 19	Trial 20
YOLOv12	n	n	n	n	n	n	n	n	n	n
- image size	1280	1600	640	640	640	640	640	640	640	1600
- epochs	42	20	100	100	100	100	100	100	100	11
BoT-SORT	✓	✓	✓	✓	✓	✓	✓	✓	✓	✓
- track buffer	60	60	30	30	30	30	30	30	30	60
- ReID module	✗	✗	sbs_S50	sbs_R101-ibn	sbs_S50	sbs_S50	sbs_S50	sbs_S50	sbs_S50	sbs_S50
- metric learning	N/A	N/A	TripletLoss	TripletLoss	TripletLoss	CircleLoss	CircleLoss	CircleLoss	CircleLoss	CircleLoss
- epochs	N/A	N/A	8	58	60	120	60	33	17	17
Scores	0.749352	0.744046	0.647239	0.646299	0.647056	0.647290	0.647423	0.647567	0.647591	0.760874

Table 4. Comprehensive evaluation results for Track 3. Experiments are grouped into four categories: (1) varying YOLOv12 model sizes, (2) tuning BoT-SORT’s track buffer, (3) exploring input image resolutions, and (4) configuring ReID modules and training strategies. The final configuration, guided by these studies, achieves the highest score, confirming the effectiveness of our optimization.

the ID reassociation process. Group 3 investigates the impact of varying image input sizes. Both 1280 and 1600 input sizes, compared to the default 640, result in a significant performance boost. Group 4 discusses trials involving different ReID modules. Trial 13 uses the full ReID dataset, while Trials 14 through 19 are trained on a reduced ReID dataset. This group also evaluates the influence of different configurations, including changes in the ReID module structure, metric learning strategies, and the number of training epochs. From these results, we draw the following conclusions: (1) ResNet-50 from the Strong Baseline Series outperforms ResNet-101 with Instance-Batch Normalization as the backbone for the ReID module, (2) replacing Triplet Loss with CircleLoss for metric learning leads to improved performance, and (3) ReID module training tends to overfit as the number of epochs increases.

Based on all trials across the groups, we draw the following conclusions regarding score variations relative to Trial 1: (1) Model size affects performance by approximately 0.001, (2) Track buffer size influences the score by around 0.0001, (3) Image input size contributes the most signifi-

cant impact, with a score increase of about 0.1, and (4) the ReID module accounts for roughly 0.01. Leveraging these insights, Trial 20, which achieved the highest score we submitted, adopts the following configuration: YOLOv12n with an image size of 1600, trained for 11 epochs, combined with BoT-SORT-SBS-S50 equipped with CircleLoss, optimized with AdamW [24] and trained for 17 epochs.

4.4. Leaderboard Results

Based on all trials across the three tracks, as summarized in Tab. 3 and Tab. 4, we report the leaderboard results in Tab. 5, which includes the top three scores for each track, our submitted scores, and the official baseline scores. While there remains a gap between our scores and the top three, 0.1332, 0.1971, and 0.0502 for Tracks 1, 2, and 3, respectively, our performance shows substantial improvement over the baselines. Specifically, we achieve approximately a twofold increase over the baseline scores in Tracks 1 and 3 and nearly a fivefold improvement in Track 2. Notably, these results were obtained without employing image enhancement techniques or leveraging temporal information during train-

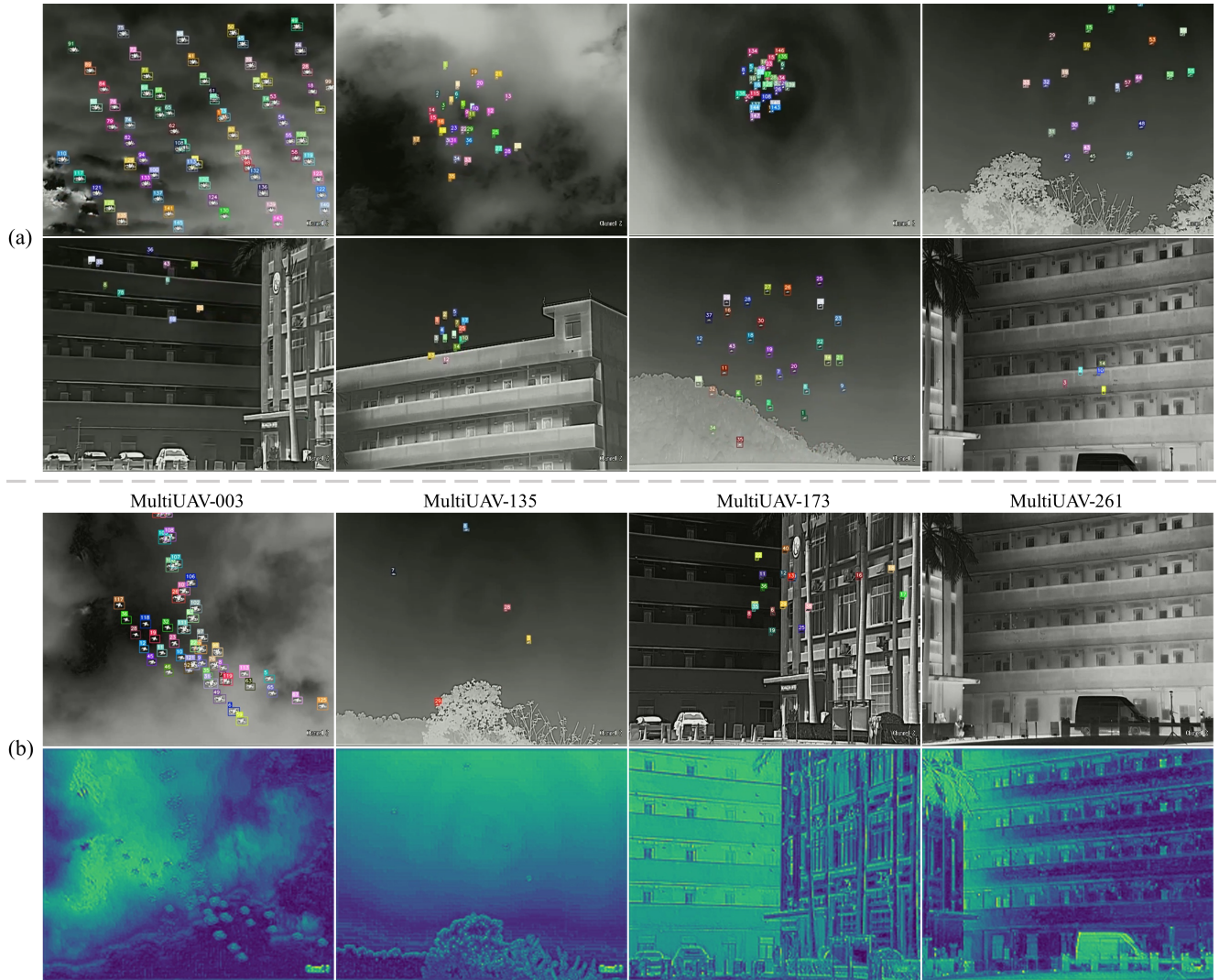


Figure 4. Demonstration of YOLOv12n with BoT-SORT-SBS-S50 predictions on Track 3 test data. (a) Predicted bounding boxes with object IDs. (b) Challenging scenarios: MultiUAV-0003 contains multiple overlapping UAVs; MultiUAV-135 includes an occluded UAV (red box, ID: 29) and a flying creature misclassified as a UAV (pink box, ID: 28); MultiUAV-173 features a complex background, where IDs 16, 17, and 18 are misjudgments; and MultiUAV-261 presents nearly invisible UAVs, leading to missed detections and tracking failures. The last row presents heatmaps highlighting the model’s difficulty in UAV perception, especially in MultiUAV-261.

ing. Integrating such advanced techniques from our strong baseline could significantly improve performance and make reaching a top-three position highly feasible.

4.5. Discussion and Enhancement Techniques

The evaluation results reveal several key insights. First, overfitting emerged due to our data-splitting strategy. To maximize scene diversity, we did not categorize videos by attributes such as fixed-camera setups or background types (*e.g.*, sky or buildings). Instead, we directly split the dataset into training, validation, and testing sets, occasionally allowing frames from the same video to appear across splits. This likely contributed to overfitting, as evidenced by AP

score discrepancies during local testing. Second, accurately rescaling the provided initial object positions to match the resolution used in training and inference is critical, as mismatches can mislead the tracker and degrade subsequent predictions. Third, increasing image resolution is key to breaking performance plateaus when parameter tuning fails to improve accuracy. For example, scaling from 640 to 1280 resolution yielded a significant score improvement of approximately 0.1. However, further increases produced diminishing gains as training at 2560 pixels for 7 epochs reached a score of 0.7072, and training at 3840 pixels for 1 epoch reached 0.7098, while both required significantly higher computational costs compared to training at 1280

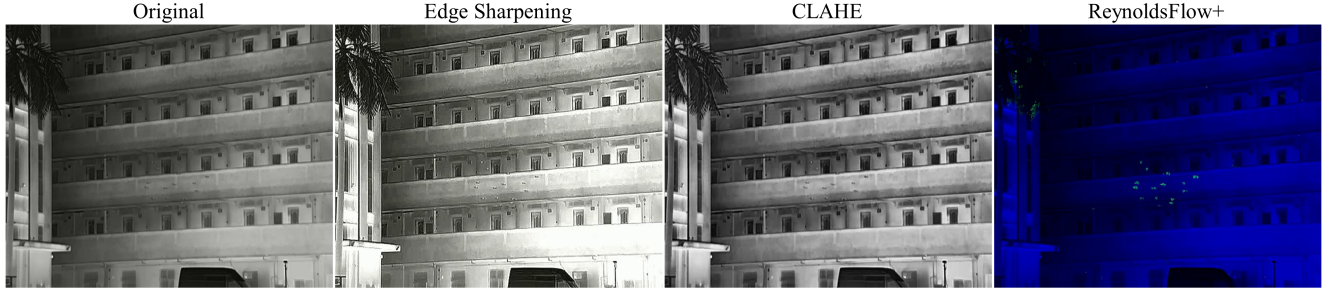


Figure 5. Potential frame enhancement techniques for multi-UAV tracking on a MultiUAV-262 video frame. From left to right: (1) original thermal infrared frame, (2) Sobel edge-based sharpening [10], (3) contrast enhancement via Contrast Limited Adaptive Histogram Equalization (CLAHE) [28], and (4) ReynoldsFlow+ visualization highlighting motion patterns to assist UAV detection [4].

Teams	Track 1	Track 2	Track 3
1st Place Team	0.7323	0.6676	0.8499
2nd Place Team	0.7308	0.5712	0.8132
3rd Place Team	0.7145	0.5530	0.8111
Strong Baseline (ours)	0.5813	0.3559	0.7609
The_4th_Anti_UAV_Baseline	0.2965	0.0745	0.3747

Table 5. Leaderboard results for the top three teams, our approach, and the official baseline across all three tracks. Our method achieved scores of 0.5813 (19th), 0.3559 (14th), and 0.7609 (5th) in Tracks 1, 2, and 3, respectively, while the official baseline scored 0.2965 (32nd), 0.0745 (20th), and 0.3747 (20th).

pixels. Fourth, memory consumption during inference with YOLOv12 and BoT-SORT-ReID accumulates over time, leading to program crashes. To address this, we executed inference on a per-folder basis rather than processing all sequences in a single run. Finally, there is a clear performance gap between runs with accurate initial object positions and those without, as reflected in the performance difference between Track 1 and Track 2. This underscores the importance of promptly and reliably estimating initial positions to boost performance further.

Additionally, as previously discussed, while our approach provides a strong baseline, it remains insufficient for achieving top-tier performance without further refinement. Fig. 4 (a) displays our model’s predictions across various scenarios, while Fig. 4 (b) highlights several key failure cases: (1) overlapping UAVs frequently cause ID switches, (2) distinguishing UAVs from flying creatures remains difficult, with the model often reassigning new IDs to UAVs following brief occlusions, (3) complex backgrounds lead to missed detections and tracking failures, and (4) tiny UAVs in cluttered environments provide little to no valuable information, making detection highly unreliable. The corresponding heatmaps in the last row illustrate the model’s inability to perceive UAVs effectively in these challenging conditions. These limitations emphasize

the importance of image enhancement techniques to improve performance further. Fig. 5 illustrates several potential image enhancement methods. From left to right: (1) the original thermal infrared frame, (2) Sobel edge-based sharpening [10], which highlights edges more clearly than the original, (3) Contrast Limited Adaptive Histogram Equalization (CLAHE) [28], which improves contrast, and (4) ReynoldsFlow+ [4], a temporal enhancement method based on the Reynolds Transport Theorem [31], a three-dimensional generalization of the Leibniz integral rule [9], providing enhanced appearance for moving UAVs.

5. Conclusion

This paper presents a strong baseline for thermal infrared video-based multi-UAV tracking tasks. By integrating YOLOv12 with BoT-SORT, our approach significantly improves over the baseline. With additional strategies during training and inference, as discussed in the experimental results, we show that our method has the potential to rank in the top three, as seen in the Track 3 performance. We also identify key factors influencing performance compared to our initial trial: model size contributing approximately 0.001, track buffer size affecting the score by around 0.0001, image input size providing the most significant impact with a score increase of about 0.1, and the ReID module adding roughly 0.01. While our approach is intuitive and straightforward, we propose several potential techniques for further improving accuracy. Overall, our method establishes a strong baseline, primarily driven by the latest YOLOv12 detector and the advanced BoT-SORT tracking algorithm, making a strong starting point in recent advancements in the UAV swarm tracking field.

6. Acknowledgments

We thank the HPC system [27] at The University of Melbourne for providing the computational resources that significantly accelerated model training and enabled the completion of this paper.

References

- [1] Nir Aharon, Roy Orfaig, and Ben-Zion Bobrovsky. Bot-sort: Robust associations multi-pedestrian tracking. *arXiv preprint arXiv:2206.14651*, 2022. 1, 3, 5
- [2] Jean-Yves Bouguet et al. Pyramidal implementation of the affine lucas kanade feature tracker description of the algorithm. *Intel corporation*, 5(1-10):4, 2001. 3
- [3] Yu-Hsi Chen. Uavdb: Trajectory-guided adaptable bounding boxes for uav detection. *arXiv preprint arXiv:2409.06490*, 2024. 1, 3
- [4] Yu-Hsi Chen and Chin-Tien Wu. Reynoldsflow: Exquisite flow estimation via reynolds transport theorem. *arXiv preprint arXiv:2503.04500*, 2025. 8
- [5] Tri Dao. Flashattention-2: Faster attention with better parallelism and work partitioning. *arXiv preprint arXiv:2307.08691*, 2023. 3
- [6] Tri Dao, Dan Fu, Stefano Ermon, Atri Rudra, and Christopher Ré. Flashattention: Fast and memory-efficient exact attention with io-awareness. *Advances in neural information processing systems*, 35:16344–16359, 2022. 3
- [7] Houzhang Fang, Xiaolin Wang, Zikai Liao, Yi Chang, and Luxin Yan. A real-time anti-distractor infrared uav tracker with channel feature refinement module. In *Proceedings of the IEEE/CVF International Conference on Computer Vision*, pages 1240–1248, 2021. 3
- [8] MA FISCHLER AND. Random sample consensus: a paradigm for model fitting with applications to image analysis and automated cartography. *Commun. ACM*, 24(6):381–395, 1981. 3
- [9] Harley Flanders. Differentiation under the integral sign. *The American Mathematical Monthly*, 80(6):615–627, 1973. 8
- [10] Suneet Gupta and Rabins Porwal. Combining laplacian and sobel gradient for greater sharpening. *IJIVP*, 6:1239–1243, 2016. 8
- [11] Ruian He, Shili Zhou, Ri Cheng, Yuqi Sun, Weimin Tan, and Bo Yan. Motion matters: Difference-based multi-scale learning for infrared uav detection. In *Proceedings of the IEEE/CVF Conference on Computer Vision and Pattern Recognition*, pages 3006–3015, 2023. 3
- [12] Bo Huang, Junjie Chen, Tingfa Xu, Ying Wang, Shenwang Jiang, Yuncheng Wang, Lei Wang, and Jianan Li. Siamsta: Spatio-temporal attention based siamese tracker for tracking uavs. In *Proceedings of the IEEE/CVF international conference on computer vision*, pages 1204–1212, 2021. 3
- [13] Bo Huang, Jianan Li, Junjie Chen, Gang Wang, Jian Zhao, and Tingfa Xu. Anti-uav410: A thermal infrared benchmark and customized scheme for tracking drones in the wild. *IEEE Transactions on Pattern Analysis and Machine Intelligence*, 46(5):2852–2865, 2023. 1
- [14] Seobin Hwang, Hanyoung Kim, Chaeyeon Heo, Youkyoung Na, Cheongeun Lee, and Yeongjun Cho. 3d trajectory reconstruction of drones using a single camera. *arXiv preprint arXiv:2309.02801*, 2023. 1
- [15] Kutalmis Gokalp Ince, Aybora Koksall, Arda Fazla, and A Aydin Alatan. Semi-automatic annotation for visual object tracking. In *Proceedings of the IEEE/CVF international conference on computer vision*, pages 1233–1239, 2021. 2
- [16] Brian KS Isaac-Medina, Matt Poyser, Daniel Organisciak, Chris G Willcocks, Toby P Breckon, and Hubert PH Shum. Unmanned aerial vehicle visual detection and tracking using deep neural networks: A performance benchmark. In *Proceedings of the IEEE/CVF International Conference on Computer Vision*, pages 1223–1232, 2021. 2
- [17] Nan Jiang, Kuiran Wang, Xiaoke Peng, Xuehui Yu, Qiang Wang, Junliang Xing, Guorong Li, Guodong Guo, Qixiang Ye, Jianbin Jiao, et al. Anti-uav: A large-scale benchmark for vision-based uav tracking. *IEEE Transactions on Multimedia*, 25:486–500, 2021. 1
- [18] Glenn Jocher, Alex Stoken, Jirka Borovec, Liu Changyu, Adam Hogan, Laurentiu Diaconu, Jake Poznanski, Lijun Yu, Prashant Rai, Russ Ferriday, et al. ultralytics/yolov5: v3. 0. *Zenodo*, 2020. 1
- [19] Aybora Koksall, Kutalmis Gokalp Ince, and Aydin Alatan. Effect of annotation errors on drone detection with yolov3. In *Proceedings of the IEEE/CVF Conference on Computer Vision and Pattern Recognition Workshops*, pages 1030–1031, 2020. 2
- [20] Jing Li, Dong Hye Ye, Timothy Chung, Mathias Kolsch, Juan Wachs, and Charles Bouman. Multi-target detection and tracking from a single camera in unmanned aerial vehicles (uavs). In *2016 IEEE/RSJ international conference on intelligent robots and systems (IROS)*, pages 4992–4997. IEEE, 2016. 1
- [21] Jingtong Li, Jesse Murray, Dorina Ismaili, Konrad Schindler, and Cenek Albl. Reconstruction of 3d flight trajectories from ad-hoc camera networks. In *2020 IEEE/RSJ International Conference on Intelligent Robots and Systems (IROS)*, pages 1621–1628. IEEE, 2020. 1
- [22] Yifan Li, Dian Yuan, Meng Sun, Hongyu Wang, Xiaotao Liu, and Jing Liu. A global-local tracking framework driven by both motion and appearance for infrared anti-uav. In *Proceedings of the IEEE/CVF Conference on Computer Vision and Pattern Recognition*, pages 3026–3035, 2023. 3
- [23] Ziming Liu, Guangyu Gao, Lin Sun, and Li Fang. Ipg-net: Image pyramid guidance network for small object detection. In *Proceedings of the IEEE/CVF conference on computer vision and pattern recognition workshops*, pages 1026–1027, 2020. 2
- [24] Ilya Loshchilov and Frank Hutter. Decoupled weight decay regularization, 2019. 6
- [25] Hao Luo, Youzhi Gu, Xingyu Liao, Shenqi Lai, and Wei Jiang. Bag of tricks and a strong baseline for deep person re-identification. In *Proceedings of the IEEE/CVF conference on computer vision and pattern recognition workshops*, pages 0–0, 2019. 4
- [26] Yanyi Lyu, Zhunga Liu, Huandong Li, Dongxiu Guo, and Yimin Fu. A real-time and lightweight method for tiny airborne object detection. In *Proceedings of the IEEE/CVF Conference on Computer Vision and Pattern Recognition*, pages 3016–3025, 2023. 3
- [27] Bernard Meade, Lev Lafayette, Greg Sauter, and Daniel Tosello. Spartan hpc-cloud hybrid: delivering performance and flexibility. *University of Melbourne*, 10:49, 2017. 5, 8
- [28] Purnawarman Musa, Farid Al Rafi, and Missa Lamsani. A review: Contrast-limited adaptive histogram equalization

- (clahe) methods to help the application of face recognition. In *2018 third international conference on informatics and computing (ICIC)*, pages 1–6. IEEE, 2018. 8
- [29] Frederik Falk Nyboe, Nicolaj Haarhøj Malle, and Emad Ebeid. Mpsoc4drones: An open framework for ros2, px4, and fpga integration. In *2022 international conference on unmanned aircraft systems (ICUAS)*, pages 1246–1255. IEEE, 2022. 1
- [30] Maciej Pawełczyk and Marek Wojtyra. Real world object detection dataset for quadcopter unmanned aerial vehicle detection. *IEEE Access*, 8:174394–174409, 2020. 1
- [31] M.C. Potter and J.F. Foss. *Fluid Mechanics*. John Wiley & Sons Canada, Limited, 1975. 8
- [32] AWS Open Data Registry. Airborne object tracking dataset, 2023. Accessed: Feb. 19, 2025. 1
- [33] Jianbo Shi et al. Good features to track. In *1994 Proceedings of IEEE conference on computer vision and pattern recognition*, pages 593–600. IEEE, 1994. 3
- [34] Daniel Steininger, Verena Widhalm, Julia Simon, Andreas Kriegler, and Christoph Sulzbachner. The aircraft context dataset: Understanding and optimizing data variability in aerial domains. In *Proceedings of the IEEE/CVF International Conference on Computer Vision*, pages 3823–3832, 2021. 1
- [35] Zongheng Tang, Yulu Gao, Zizheng Xun, Fengguang Peng, Yifan Sun, Si Liu, and Bo Li. Strong detector with simple tracker. In *Proceedings of the IEEE/CVF Conference on Computer Vision and Pattern Recognition*, pages 3047–3053, 2023. 3
- [36] Yunjie Tian, Qixiang Ye, and David Doermann. Yolov12: Attention-centric real-time object detectors. *arXiv preprint arXiv:2502.12524*, 2025. 1, 3
- [37] Chien-Yao Wang, Alexey Bochkovskiy, and Hong-Yuan Mark Liao. Yolov7: Trainable bag-of-freebies sets new state-of-the-art for real-time object detectors. In *Proceedings of the IEEE/CVF conference on computer vision and pattern recognition*, pages 7464–7475, 2023. 3
- [38] Guanshuo Wang, Yufeng Yuan, Xiong Chen, Jiwei Li, and Xi Zhou. Learning discriminative features with multiple granularities for person re-identification. In *Proceedings of the 26th ACM international conference on Multimedia*, pages 274–282, 2018. 4
- [39] Zixuan Wang, Zhicheng Zhao, and Fei Su. Real-time tracking with stabilized frame. In *Proceedings of the IEEE/CVF Conference on Computer Vision and Pattern Recognition Workshops*, pages 1028–1029, 2020. 3
- [40] Nicolai Wojke, Alex Bewley, and Dietrich Paulus. Simple online and realtime tracking with a deep association metric. In *2017 IEEE international conference on image processing (ICIP)*, pages 3645–3649. IEEE, 2017. 1, 3
- [41] Han Wu, Weiqiang Li, Wanqi Li, and Guizhong Liu. A real-time robust approach for tracking uavs in infrared videos. In *Proceedings of the IEEE/CVF Conference on Computer Vision and Pattern Recognition Workshops*, pages 1032–1033, 2020. 3
- [42] Xin Yang, Gang Wang, Weiming Hu, Jin Gao, Shubo Lin, Liang Li, Kai Gao, and Yizheng Wang. Video tiny-object detection guided by the spatial-temporal motion information. In *Proceedings of the IEEE/CVF conference on computer vision and pattern recognition*, pages 3054–3063, 2023. 3
- [43] Mang Ye, Jianbing Shen, Gaojie Lin, Tao Xiang, Ling Shao, and Steven CH Hoi. Deep learning for person re-identification: A survey and outlook. *IEEE transactions on pattern analysis and machine intelligence*, 44(6):2872–2893, 2021. 3
- [44] Qianjin Yu, Yinchao Ma, Jianfeng He, Dawei Yang, and Tianzhu Zhang. A unified transformer based tracker for anti-uav tracking. In *Proceedings of the IEEE/CVF Conference on Computer Vision and Pattern Recognition*, pages 3036–3046, 2023. 3
- [45] Yifu Zhang, Peize Sun, Yi Jiang, Dongdong Yu, Fucheng Weng, Zehuan Yuan, Ping Luo, Wenyu Liu, and Xinggang Wang. Bytetrack: Multi-object tracking by associating every detection box. In *European conference on computer vision*, pages 1–21. Springer, 2022. 4
- [46] Jinjian Zhao, Xiaohan Zhang, and Pengyu Zhang. A unified approach for tracking uavs in infrared. In *Proceedings of the IEEE/CVF International Conference on Computer Vision*, pages 1213–1222, 2021. 3